

## TERRAIN ROUGHNESS PARAMETERS FROM FULL-WAVEFORM AIRBORNE LIDAR DATA

M. Hollaus<sup>a,\*</sup>, B. Höfle<sup>b</sup>

<sup>a</sup> Institute of Photogrammetry & Remote Sensing, Vienna University of Technology,

Gußhausstr. 27-29, A-1040 Vienna, Austria, mh@ipf.tuwien.ac.at

<sup>b</sup> Department of Geography, University of Heidelberg, Berliner Str. 48, D-69120 Heidelberg, Germany, hoefle@uni-heidelberg.de

**KEY WORDS:** Three-dimensional, LIDAR, Surface, DEM/DTM, Retrieval, Geomorphology, Roughness

### ABSTRACT:

As an active remote sensing technique airborne laser scanning (ALS) is able to capture the topography with high precision even for densely forested areas. Due to the high pulse repetition frequency of up to 400 kHz a high sampling rate on the ground can be achieved, which allows the description of the terrain surface in decimeter scale. In this contribution two approaches to characterize terrain roughness are described. In the first approach the standard deviation of detrended terrain points is calculated. To achieve a high spatial resolution of the derived roughness layer a high terrain point density is essential, which requires especially in dense forested areas a very high sampling rate. In addition to the 3D position of backscattering objects, full-waveform ALS systems provide the width of each detectable echo, which provides information on the range distribution of scatterers within the laser footprint that contribute to one echo. It is therefore, an indicator for surface roughness and the slope of the target. In comparison to the roughness layer derived from the first approach using high point densities, the derived echo width image shows similar spatial patterns of terrain roughness even for moderate point densities. The results show that both the echo widths and the vertical distribution of terrain echoes are useful to derive reliable geometric terrain roughness layers of large areas.

### 1. INTRODUCTION

For the modeling of natural hazards e.g. avalanches (e.g. Margreth and Funk, 1999), rock falls (e.g. Dorren and Heuvelink, 2004) and floods (e.g. Govers et al., 2000), information about the terrain roughness is required. For these different natural processes different levels of detail of the terrain roughness from micro-level (e.g. millimeters to centimeters), to meso-level (e.g. decimeter to meters) to macro-level (e.g. meter to kilometers) are required. For practical applications the terrain roughness is commonly estimated by field investigations, which are typically based on thematic roughness classes as for example described by Markart et al. (2004). Furthermore, the terrain or landscape roughness in the macro-level can be determined from digital terrain model (DTM) analyses as for example shown in Smith et al. (2004). Also for the meso-level investigations exist that use airborne laser scanning (ALS) and spectral remote sensing data for floodplain roughness parameterization (e.g. Straatsma and Baptist, 2008).

Especially for forested areas ALS, also referred to as LiDAR, has been proven as the state of the art technology for the acquisition of topographic information. As an active remote sensing technique ALS is able to capture the topography with high precision even for densely forested areas. The transmitted nanosecond-long (e.g. 4 ns) laser pulses in the near-infrared range of wavelengths (e.g. 1.0 or 1.5  $\mu\text{m}$ ) have a typical beam

divergence of 0.5 mrad, resulting in footprint diameters of 0.2 to 0.5 m for typical flying heights above ground of 400 to 1000 m. Due to the high pulse repetition frequency of up to 400 kHz a high sampling rate on the ground can be achieved, which allows the description of the terrain surface in decimeter scale.

In this contribution two approaches to characterize terrain roughness with geometric quantities are described. In the first approach the standard deviation of detrended terrain points is calculated. To achieve a high spatial resolution (e.g. 1.0 x 1.0 m) of the derived roughness layer a high terrain point density is required. Especially in dense forested areas where the laser beam penetration rates can decrease to 10% to 20% (e.g. Hollaus et al., 2006) a very high sampling rate is, therefore, mandatory. In addition to the 3D position of backscattering objects, full-waveform (FWF) ALS systems provide (i) the signal amplitude characterizing the reflectance of the scanned surface and (ii) the width of each detectable echo, which provides information on the range distribution of scatterers within the laser footprint that contribute to one echo (Wagner et al., 2004). Consequently, it is assumed that the echo width is an indicator for roughness and the slope of the target. Thus, in the second approach the potential of the derived echo widths are analysed for terrain roughness characterization. Finally, both derived terrain roughness layers are compared and discussed.

\* Corresponding author.

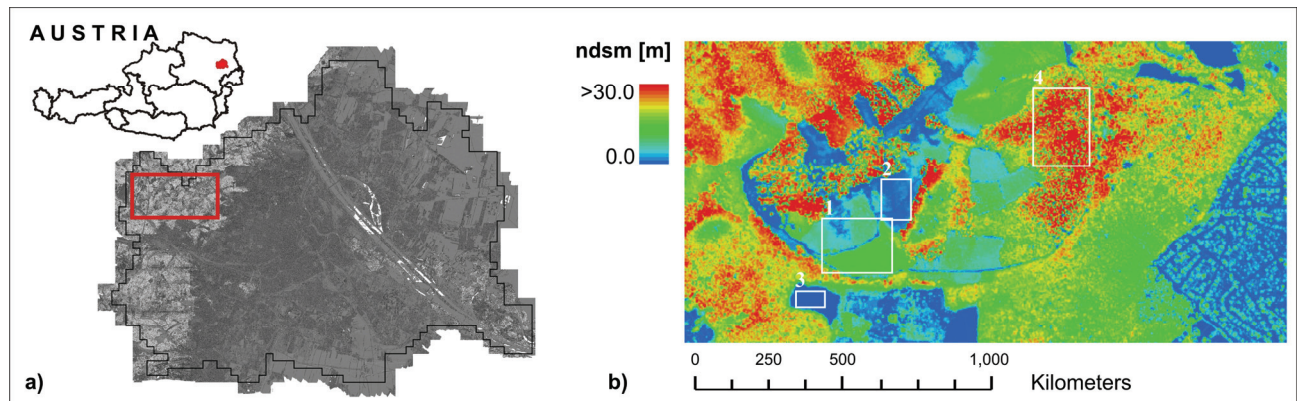


Figure 1. Overview of the study area: a) digital surface model of the city of Vienna, b) normalized digital surface model (nDSM) of the study area in the Vienna Woods. In the subareas 1-4 additional analyses are done (see Sect. 3.3).

## 2. STUDY AREA AND DATA

The study area is located in the western part of Vienna (Fig. 1), in the so-called Vienna Woods, and covers about 200 hectares forest and a small part of an urban area. The study area is part of the UNESCO biosphere reserve Wienerwald<sup>1</sup>, which was installed by the provinces of Lower Austria and Vienna in 2005. Since the 19<sup>th</sup> century the Wienerwald region has been used as a traditional recreation area for Viennese and inhabitants of Lower Austria, which are living in the immediate vicinity. In general, the landscape of the Vienna wood is characterized by individual deciduous forests, which are closely interlinked with meadows while the forests are dominated by oak and hornbeam, beech at higher altitudes, and ash in the peak region of north-facing slopes. Within the investigated area the dominating tree species are red beech (*Fagus sylvatica*) with ~51%, oaks (*Quercus robur*, *Quercus petraea*) with ~23% and hornbeam (*Carpinus betulus*) with ~16%. The remaining areas are covered with ~6% larch (*Larix decidua*), 2% clearings and other deciduous and coniferous tree species. The forests are characterized by a balanced age class distribution (tree ages vary between 5 and 180 years) and with tree heights varying between 2.0 m and 45.0 m. The clearings are partly covered by very dense brushwood i.e. blackberry. Furthermore, some young forest stands covered with very dense red beech (*Fagus sylvatica*) are available.

For the study area full-waveform airborne laser scanning (FWF-ALS) data was provided by the city of Vienna (MA41 Stadtvermessung) and was acquired in the framework of a commercial terrain mapping project, fully covering the city of Vienna. The FWF-ALS data was acquired with a Riegl LMS-Q560 by the company Diamond Airborne Sensing<sup>2</sup> in cooperation with AREA Vermessung ZT GmbH<sup>3</sup> in January 2007. The average point density is greater than 30 echoes per square meter. The pre-processing of the FWF-ALS data was done from the company AREA Vermessung ZT GmbH using the Riegl software packages<sup>4</sup>. For the current study the geo-referenced 3D echo points and the determined attributes for each echo, i.e. the echo width and the amplitude, serve as input for the following analyses.

The digital terrain model (DTM) was calculated using the SCOP++ (2010) software. For the determination of the digital surface model (DSM) the approach described in Hollaus et al. (2010) was applied using the OPALS (2010) software. Finally, the normalized digital surface model (nDSM) was calculated by subtracting the DTM from the DSM (cf. Fig. 1b). The derived topographic models (DTM, DSM, nDSM) have a spatial resolution of 0.5 m. The DTM is used for normalizing the 3D echo points (dz) and therefore, for the selection of terrain and near-terrain echoes (cf. Sect. 3.1 and 3.2). The nDSM is used for visualization purposes only.

## 3. TERRAIN ROUGHNESS PARAMETERS FROM FWF-ALS DATA

Looking at roughness from the ALS sensing technique point of view (Fig. 2), the spatial scale of observation plays a crucial role. Roughness with a spatial scale of up to a few decimeters cannot be determined directly by using the ALS range measurements (i.e. XYZ of point cloud) because of the range accuracy (Kraus, 2007), which generally lies far above the given laser wavelength of a few micrometers. Hence, micro structures can only be determined indirectly, for example, by using the strength of reflection of a laser echo (i.e. amplitude), which is correlated with target reflectivity but also surface roughness (Wagner et al., 2004).

Macro structure  $> d$        $d >$  Meso structure  $\gg \lambda$        $\lambda >$  Micro structure

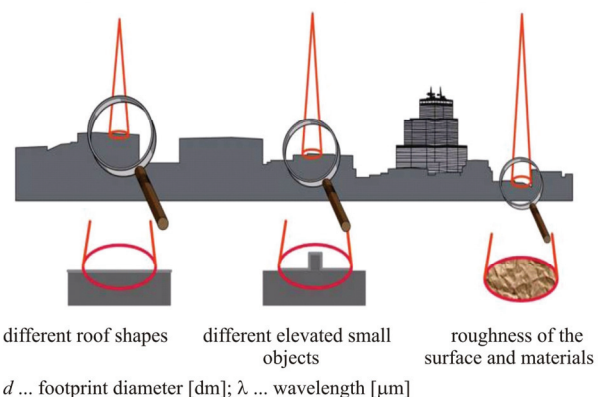


Figure 2. Scales of roughness in terms of the ALS sensing technique (modified from Jutzi and Stilla, 2005).

<sup>1</sup> <http://www.biosphaerenpark-wienerwald.org>

<sup>2</sup> <http://www.diamond-air.at/airbornesensing.html>

<sup>3</sup> <http://www.area-vermessung.at/>

<sup>4</sup> <http://www.riegl.com/nc/products/airborne-scanning/>

The focus of the current paper is on the terrain roughness parameterization of the meso structure (Fig. 2). For the parameterization of the terrain roughness two approaches are investigated. In the first approach a geometric description by calculating the standard deviation of detrended terrain points is used. In the second approach the potential of the derived echo widths are analyzed for terrain roughness characterization.

### 3.1 Standard deviation of detrended terrain points

In this first approach the terrain roughness is parameterized by the standard deviation of the detrended z-coordinates of all FWF-ALS echoes within a raster cell or a certain distance of e.g. 1.0 m, which are located below a defined normalized height (dz) threshold (Fig. 3a). For the current study four different height thresholds (0.25 m, 0.5 m, 1.0 m, 2.0 m) are applied. The detrending of the FWF-ALS heights is important for slanted surfaces, where else the computed standard deviation would increase with increasing slope (i.e. height variation), even though the surface is plane. Algorithmically, simply the standard deviation of orthogonal regression plane fitting residuals is chosen. Taking the residuals to a best fit plane can be compared to a prior detrending of the heights. The orthogonal regression plane fitting (Fig. 3b) is favored over vertical fitting because for very steep surfaces the vertical residuals can become very large, even though the plane fits very well to the points. In this sense orthogonal fitting means that the orthogonal distances from plane to points is minimized. In practical, for every laser echo the orthogonal plane fitting is performed in a local neighborhood (i.e. considering all terrain echo neighbors in a certain distance for plane computation; e.g. <math><1.0\text{ m}</math>) and stored as additional attribute to the original laser echo.

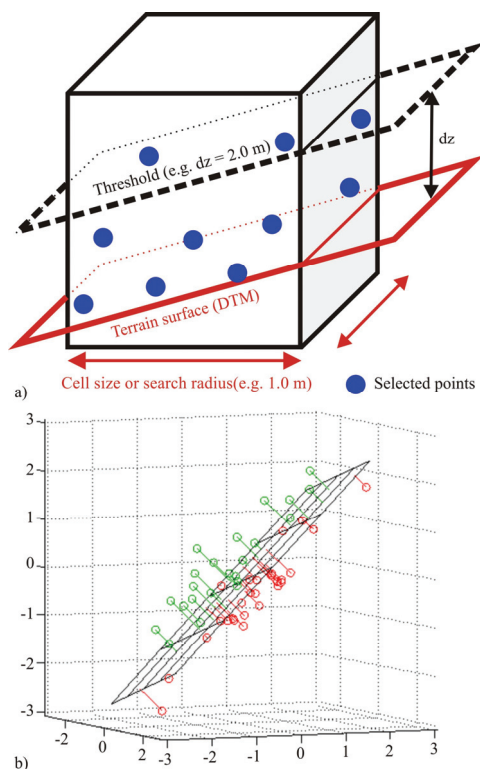


Figure 3. Standard deviation of detrended terrain points: a) Predefined cube or cylinder for selecting echoes used for plane fitting. b) Principle of orthogonal regression plane fitting (modified from [www.mathworks.com](http://www.mathworks.com)).

The unit of the so derived terrain roughness parameter is in meters and can be compared between different flight epochs and ALS systems. Finally, the derived standard deviations are averaged per raster cell.

### 3.2 Echo width of terrain points

The meso structure is defined to be smaller than the footprint diameter (Fig. 2). Such structures can be obtained either directly, if a high point density with overlapping footprints is given or the range resolution of the scanner system allows distinguishing multiple echoes in the magnitude of few decimeters, which is currently not achieved by state-of-the-art scanners. The maximum sampling interval is currently 1.0 ns, which corresponds to approx. 15.0 cm (30.0 cm for both ways) (Wagner et al., 2006). For objects few times larger than the sampling interval, the widening of the echo (i.e. larger echo width) indicates a certain vertical extent of the illuminated object, which can be assigned to roughness in a broader sense. For the used FWF-ALS data the received full-waveforms were digitized with an interval of 1 ns (Fig. 4). A Gaussian decomposition method was applied to estimate in addition to the location the scattering properties of the targets i.e. the amplitude and the echo width (Wagner et al., 2006). Therefore, the derived echo width of each single echo is representative for the roughness within the illuminated footprint (Fig. 4). For deriving the terrain roughness layer laser points within a maximal vertical distance (dz) to the DTM (dz = 0.25 m, 0.5 m, 1.0 m, 2.0 m) are selected. For a laser beam with multiple echoes the illuminated footprint decreases depending on the collision area of the previous reflected echoes. Only single echoes are selected for the terrain roughness parameterization, in order to guarantee that only extended targets with similar footprint sizes are investigated. For this study the influence of varying flying heights and consequently to varying ranges, and the local incidence angle are neglected. Finally the terrain roughness layers are generated by aggregating the selected echo widths per raster cell (e.g. mean value). The unit of the terrain roughness layers is in nanoseconds and could be converted to meters.

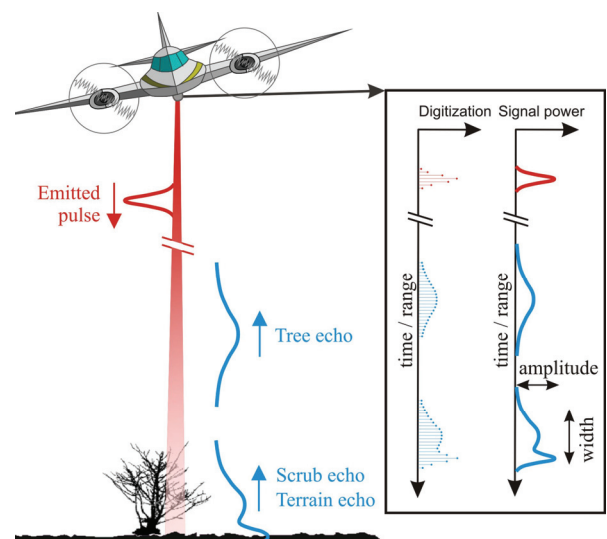


Figure 4. Full-waveform ALS system. A Gaussian decomposition is applied to derive echo widths, which are used for the parameterization of terrain roughness. (adapted from Doneus et al., 2008)

### 3.3 Validation of the terrain roughness parameters

In a first processing step the derived terrain roughness layers (standard deviation of detrended terrain points, mean echo widths of terrain points) are compared. A linear regression from both roughness images, according to the formula  $y = a + b \cdot x$ , where  $x$  and  $y$  represent raster maps was calculated. In addition to the entire image, subareas were selected, each representing an individual land cover type (see subareas in Fig. 1) i.e. grass (3), bushes (2), young (1) and old (4) forest for calculating the linear regression. Finally, a plausibility check was done by field investigations. Furthermore, the effect of varying footprint sizes caused by multiple echoes on the derived echo widths is studied. To ensure, that only echoes with footprint sizes, which are in a similar range, are used, only single echoes (i.e. extended targets) that are below the defined height thresholds were selected. The selected single echoes are used to generate additional roughness layers.

### 4. RESULTS AND DISCUSSION

Fig. 5 shows the standard deviation of the detrended terrain points as well as mean echo widths of using all echoes. High standard derivations (bright areas) indicate a high terrain roughness. Large echo widths (bright areas) are caused by a certain vertical distribution of scatterers within a laser shot footprint and hence large echo widths indicate high terrain roughness. The visual comparison of the derived roughness layers (Fig. 5) clearly shows similar spatial patterns of areas with high values of terrain roughness. It can also be shown that this similarity is apparent for all applied height thresholds. The highest correlation coefficients ( $R=0.62 - 0.63$ ) are available for the roughness layers derived from echoes with heights ( $dz$ ) less than 0.25 m and 0.50 m, respectively. The linear regression between the standard deviation of the detrended terrain points and the mean echo widths derived from the extended targets show a slight decrease of the correlation coefficients e.g. for echoes with  $dz < 0.5$  m from  $R=0.63$  to  $R=0.58$ .

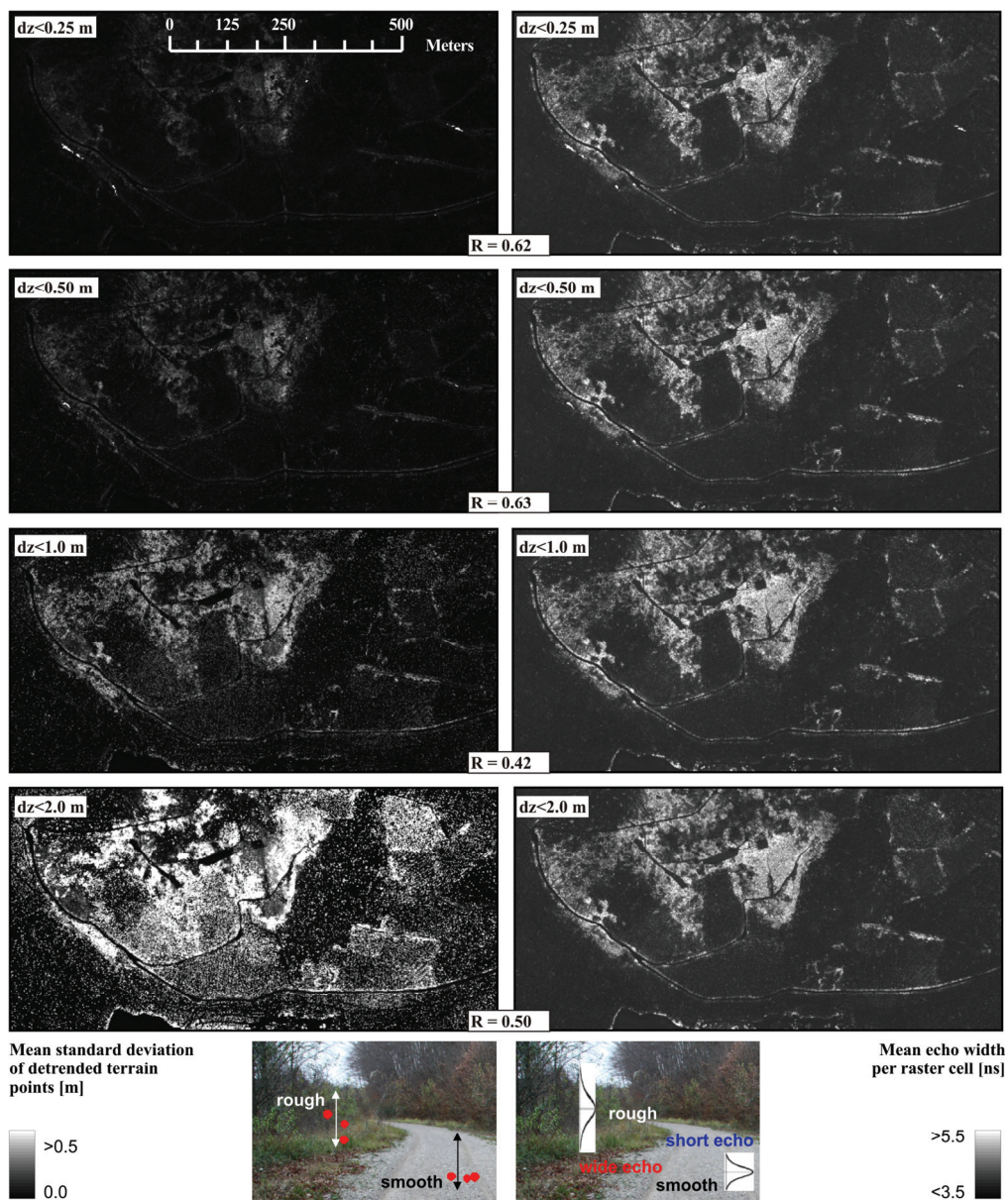


Figure 5. Roughness layers derived from FWF-ALS data. Left: Mean standard deviation per raster cell of detrended terrain points for different height thresholds. Right: Mean echo width per raster cell calculated from terrain and near terrain points respectively.



Figure 6. Shading of the standard deviation of the detrended terrain echoes ( $dz < 1.0$  m overlaid with pictures from different features).

This indicates that varying footprint sizes of single and multiple echoes have a negligible influence on the terrain roughness parameterization. For the young forest subarea (see Fig. 1, region 1) the correlation coefficients increase e.g. to 0.68 for echoes with  $dz < 0.25$  m. For all other subareas (see Fig. 1, region 2-4) the correlation coefficients decrease. However, as a decrease was not expected further statistics were calculated. For the grassland subarea the standard deviation of the mean echo width is 0.03 ns and for the old forest stand subarea the standard deviation is 0.02 ns. Also the standard deviation of the mean standard deviation per raster cell of detrended terrain points are small and are in the range of 0.4 to 1.9 centimeters. This means that there is only a constant shift between the two roughness layers. Furthermore, this indicates very homogeneous and smooth surfaces, which corresponds to the information derived during the field check. Moreover, this small standard deviations can be interpreted as measurement noise of the used FWF-ALS system. Even in the densely forested areas with FWF-ALS it is possible to acquire a sufficient amount of elevation measurements of the forest terrain surface. As shown in Fig. 6 areas indicated by high roughness values are mainly covered by low vegetation (e.g. bushes) or exhibit a very dense distribution of tree stems, which also account for terrain roughness as defined in this study. High roughness values are also available at the borders of forest roads and tracks where commonly discontinuities (e.g. breaklines) are available. The results let assume that FWF-ALS echo width values are able to identify areas with high terrain roughness without the need of a highly detailed geometrical representation of the ground surface by

acquiring very dense point clouds. However, there are still some uncertainties by using the echo width for terrain roughness parameterization. While pulse width estimates are relatively stable at high amplitudes, there is significant scattering at low amplitudes (Lin and Mills, 2010; Mücke, 2008; Wagner et al., 2006). This needs to be taken into account in future studies. Furthermore, the comparison of the derived roughness layers has shown that small (i.e. in relation to the footprint size) terrain surface discontinuities i.e. breaklines which are not covered with vegetation or stems lying on the terrain are better represented in the geometry-based roughness layer than in the mean echo width (Fig. 7). This can be explained by the small laser footprints, and therefore, by the fact that within the small illuminated area only little vertical variations are available.

## 5. CONCLUSION AND OUTLOOK

In addition to the 3D-coordinates, FWF-ALS delivers laser point attributes (e.g. signal amplitude, echo width) providing further quantities to characterize Earth surface properties. The presented analyses have shown that the FWF-ALS echo width derived roughness layer indicates areas with high roughness similarly to the geometric definition using very high laser point densities. Concluding the echo width can be used as a terrain roughness parameter even with low terrain point densities compared to the geometry-based computation.

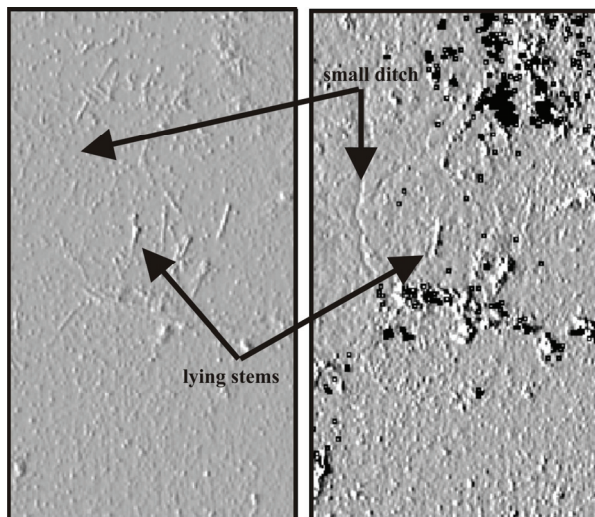


Figure 7. Shading of the geometry-based roughness (left) and of the mean echo widths (right);  $dz < 0.5$  m. Black areas are nodata raster cells.

Such roughness layers are valuable input datasets for further analyses as for example shown in Aubrecht et al. (2010) but also directly for a multitude of process models and simulations. In future research the influence of varying flying heights and incidence angles on the echo width is investigated. Furthermore, the increasing uncertainty with weak signals, resulting in low amplitudes, will be studied.

#### ACKNOWLEDGMENTS

The presented research was funded by the Austrian Research Promotion Agency (FFG) in the frame of the Austrian Space Applications Program (ASAP). The airborne laser scanning data was provided by the MA 41 Stadtvermessung, Wien.

#### REFERENCES

- Aubrecht, C., Höfle, B., Hollaus, M., Köstl, M., Steinnocher, K., Wagner, W., 2010. Vertical roughness mapping - ALS based classification of the vertical vegetation structure in forested areas. ISPRS International Archives of the Photogrammetry, Remote Sensing and Spatial Information Sciences, pp. 6, in press.
- Doneus, M., Briese, C., Fera, M. and Janner, M., 2008. Archaeological prospection of forested areas using full-waveform airborne laser scanning. *Journal of Archaeological Science* 35(4), pp. 882-893.
- Dorren, L.K.A. and Heuvelink, G.B.M., 2004. Effect of support size on the accuracy of a distributed rockfall model. *Int. J. Geographical Information Science* 18(6), pp. 595-609.
- Govers, G., Takken, I. and Helming, K., 2000. Soil roughness and overland flow. *Agronomie* 20, pp. 131-146.
- Hollaus, M., Wagner, W., Eberhöfer, C. and Karel, W., 2006. Accuracy of large-scale canopy heights derived from LiDAR data under operational constraints in a complex alpine environment. *ISPRS Journal of Photogrammetry & Remote Sensing* 60(5), pp. 323-338.
- Hollaus M., Mandlbürger G., Pfeifer N., Mücke W., 2010. Land cover dependent derivation of digital surface models from airborne laser scanning data. *International Archives of Photogrammetry, Remote Sensing and the Spatial Information Sciences*. PCV 2010, Paris, France, Vol. 39(3). pp. 6.
- Jutzi, B. and Stilla, U., 2005. Waveform processing of laser pulses for reconstruction of surfaces in urban areas. In: M. Moeller and E. Wentz (Eds.): 3th International Symposium: Remote sensing and data fusion on urban areas, URBAN 2005. *International Archives of Photogrammetry and Remote Sensing*, 36, Part 8 W27, pp. 6.
- Kraus, K., 2007. *Photogrammetry - Geometry from Images and Laser Scans*. Walter de Gruyter, Berlin, pp. 459.
- Lin, Y., Mills, JP., 2010. Factors Influencing Pulse Width of Small Footprint, Full Waveform Airborne Laser Scanning Data. *Photogrammetric Engineering & Remote Sensing* 76(1). pp. 49-59.
- Margreth, S. and Funk, M., 1999. Hazard mapping for ice and combined snow/ice avalanches - two case studies from the Swiss and Italian Alps. *Cold Regions Science and Technology* 30(1-3), pp. 159-173.
- Markart, G., Kohl, B., Sotier, B., Schauer, T., Bunza, G. and Stern, R., 2004. Provisorische Geländeanleitung zur Abschätzung des Oberflächenabflussbeiwertes auf alpinen Boden-/Vegetationseinheiten bei konvektiven Starkregen (Version 1.0). BFW-Dokumentation 3, pp. 83.
- Mücke, W., 2008. Analysis of full-waveform airborne laser scanning data for the improvement of DTM generation. Thesis, Institute of Photogrammetry and Remote Sensing, Technical University Vienna, Vienna, pp. 67.
- OPALS, 2010. Orientation and Processing of Airborne Laser Scanning Data, <http://www.ipf.tuwien.ac.at/opals/> (accessed June 2010).
- Scop++, 2010. Programpackage for Digital Terrain Models, <http://www.ipf.tuwien.ac.at/products;> <http://www.inpho.de> (accessed June 2010).
- Smith, M.J., Asal, F.F.F. and Priestnall, G., 2004. The Use of Photogrammetry and LIDAR for Landscape Roughness Estimation in Hydrodynamic Studies. *International Society for Photogrammetry and Remote Sensing XXth Congress*, Vol XXXV, WG III/8, Istanbul, Turkey, pp. 6.
- Straatsma, M.W. and Baptist, M.J., 2008. Floodplain roughness parameterization using airborne laser scanning and spectral remote sensing. *Remote Sensing of Environment* 112(3), pp. 1062-1080.
- Wagner, W., Ullrich, A., Ducic, V., Melzer, T. and Studnicka, N., 2006. Gaussian decomposition and calibration of a novel small-footprint full-waveform digitising airborne laser scanner. *ISPRS Journal of Photogrammetry & Remote Sensing* 60(2), pp. 100-112.
- Wagner, W., Ullrich, A., Melzer, T., Briese, C. and Kraus, K., 2004. From single-pulse to full-waveform airborne laser scanners: Potential and practical challenges. *International Society for Photogrammetry and Remote Sensing XXth Congress*, Vol XXXV, Part B/3, Istanbul, Turkey, pp. 6.